Publications of the Astronomical Society of the Pacific, **115**:965–980, 2003 August

From Molecular Cores to Planet-forming Disks: An *SIRTF* Legacy Program

Neal J. Evans II,[1] Lori E. Allen,[2] Geoffrey A. Blake,[3] A. C. A. Boogert,[4] Tyler Bourke,[2] Paul M. Harvey,[1] J. E. Kessler,[5] David W. Koerner,[6] Chang Won Lee,[7] Lee G. Mundy,[8] Philip C. Myers,[2] Deborah L. Padgett,[9] K. Pontoppidan,[10] Anneila I. Sargent,[4] Karl R. Stapelfeldt,[11] Ewine F. van Dishoeck,[10] Chadwick H. Young,[1] and Kaisa E. Young[1]

Received 2003 March 6; accepted 2003 April 18

ABSTRACT. Crucial steps in the formation of stars and planets can be studied only at mid- to far-infrared wavelengths, where the *Space Infrared Telescope* (*SIRTF*) provides an unprecedented improvement in sensitivity. We will use all three *SIRTF* instruments (Infrared Array Camera [IRAC], Multiband Imaging Photometer for *SIRTF* [MIPS], and Infrared Spectrograph [IRS]) to observe sources that span the evolutionary sequence from molecular cores to protoplanetary disks, encompassing a wide range of cloud masses, stellar masses, and star-forming environments. In addition to targeting about 150 known compact cores, we will survey with IRAC and MIPS (3.6–70 μm) the entire areas of five of the nearest large molecular clouds for new candidate protostars and substellar objects as faint as 0.001 solar luminosities. We will also observe with IRAC and MIPS about 190 systems likely to be in the early stages of planetary system formation (ages up to about 10 Myr), probing the evolution of the circumstellar dust, the raw material for planetary cores. Candidate planet-forming disks as small as 0.1 lunar masses will be detectable. Spectroscopy with IRS of new objects found in the surveys and of a select group of known objects will add vital information on the changing chemical and physical conditions in the disks and envelopes. The resulting data products will include catalogs of thousands of previously unknown sources, multiwavelength maps of about 20 deg^2 of molecular clouds, photometry of about 190 known young stars, spectra of at least 170 sources, ancillary data from ground-based telescopes, and new tools for analysis and modeling. These products will constitute the foundations for many follow-up studies with ground-based telescopes, as well as with *SIRTF* itself and other space missions such as *SIM*, *JWST*, *Herschel*, and *TPF/Darwin*.

1. INTRODUCTION

Stars and planets form in a closely coupled process that is generally accessible to study only at relatively long wavelengths, from infrared to radio. Observational studies of this process have generally suffered from one or more of the following problems: biased samples, inadequate sensitivity, inadequate spatial resolution, or incomplete data across the wavelength ranges of interest. The *Space Infrared Telescope Facility* (*SIRTF*) offers a singular opportunity for a major advance in this area of research. The *SIRTF* mission has been described by Gallagher, Irace, & Werner (2003).

Our Legacy program, "From Molecular Cores to Planet-forming Disks," uses 400 hr of *SIRTF* observations to study the process of star and planet formation from the earliest stages of molecular cores to the epoch of planet-forming disks. This program, hereafter referred to simply as "Cores to Disks" (c2d), is closely coordinated with the Legacy program on "Formation and Evolution of Planetary Systems" (FEPS), which carries the age sequence to later times. Our program uses all three *SIRTF* instruments: the Infrared Array Camera (IRAC), covering 3.6–8 μm (Fazio et al. 1998); the Multiband Imaging Photometer for *SIRTF* (MIPS), covering 24–160 μm (Engelbracht et al. 2000); and the Infrared Spectrometer (IRS), supplying spectroscopy from 5.3 to 40 μm with resolving power $R = 60$–120 and from 10 to 37 μm with $R = 600$ (Houck et al. 2000).

[1] Department of Astronomy, University of Texas at Austin, 1 University Station C1400, Austin, TX 78712–0259; nje@astro.as.utexas.edu, pmh@astro.as.utexas.edu, cyoung@astro.as.utexas.edu, kaisa@astro.as.utexas.edu.

[2] Smithsonian Astrophysical Observatory, 60 Garden Street, MS42, Cambridge, MA 02138; leallen@cfa.harvard.edu, tbourke@cfa.harvard.edu, pmyers@cfa.harvard.edu.

[3] Division of Geological and Planetary Sciences, MS 150-21, California Institute of Technology, Pasadena, CA 91125; gab@gps.caltech.edu.

[4] Division of Physics, Mathematics, and Astronomy, MS 105-24, California Institute of Technology, Pasadena, CA 91125; acab@astro.caltech.edu, afs@astro.caltech.edu.

[5] Division of Chemistry and Chemical Engineering, California Institute of Technology, Pasadena, CA 91125; kessler@its.caltech.edu.

[6] Department of Physics and Astronomy, Northern Arizona University, Box 6010, Flagstaff, AZ 86011-6010; koerner@physics.nau.edu.

[7] Taeduk Radio Astronomy Observatory, Korea Astronomy Observatory, 36-1 Hwaam-dong, Yusung-gu, Taejon 305-348, Korea; cwl@trao.re.kr.

[8] Department of Astronomy, University of Maryland, College Park, MD 20742; lgm@astro.umd.edu.

[9] *SIRTF* Science Center, MC 220-6, Pasadena, CA 91125; dlp@ipac.caltech.edu.

[10] Leiden Observatory, Postbus 9513, 2300 RA Leiden, Netherlands; pontoppi@strw.leidenuniv.nl, ewine@strw.leidenuniv.nl.

[11] Jet Propulsion Laboratory, MS 183-900, California Institute of Technology, 4800 Oak Grove Drive, Pasadena, CA 91109; krs@exoplanet.jpl.nasa.gov.

The observational programs, described in greater detail in the individual sections, include unbiased mapping of five large nearby molecular clouds and about 150 compact molecular cores (§ 2), photometry of about 190 stars with ages up to about 10 Myr (§ 3), and spectroscopy of at least 170 objects in a wide range of evolutionary states (§ 4). In these sections, we discuss the scientific questions, the sample selection, the planned observations, and the expected results. The data products are summarized in § 5. We also describe *ancillary* data, which are part of the c2d data products, and *complementary* data, which are being obtained by us or others to provide a more complete picture. The *SIRTF* and ancillary data will be available to the broader community from the *SIRTF* Science Center (SSC) via their Infrared Sky Archive (IRSA). Complementary data products will be made available, as far as possible, through either IRSA or public Web sites. Further information on the program can be found at the c2d Web site.[12]

2. A SURVEY OF NEARBY MOLECULAR CLOUDS AND CORES

2.1. Scientific Questions

The *SIRTF* mission offers an unprecedented opportunity to determine the stellar content of the nearest star-forming molecular clouds, the distributions of their youngest stars and substellar objects, and the properties of their circumstellar envelopes and disks. Just as *IRAS* and *ISO* revealed many properties of isolated and clustered star-forming regions, *SIRTF* will yield new insights into how stars and brown dwarfs are born. Among the specific questions that our program will address are the following:

1. In large cloud complexes, how are the youngest stars and substellar objects distributed, in position and mass? The IRAC and MIPS maps of large complexes will reveal the reddest, and presumably youngest, associated objects. Is their distribution "bimodal" between singles and clusters, or is there a more continuous distribution of multiplicity? Is the distribution of young stars better correlated with line-of-sight extinction, the supply of dense gas, or with proximity to other young stars, a measure of triggering or cooperative star formation? Do the answers to these questions depend on the mass of the object—for example, can brown dwarfs form in isolation, as can ordinary low-mass stars, or do they require proximity to stars, as expected if they originate primarily in circumstellar disks or in small stellar groups?

2. What is the incidence of circumstellar disks in complexes and in isolated cores? The excess emission over that of a stellar photosphere at near- and mid-infrared wavelengths indicates the presence of a circumstellar disk, the birthplace of planets. To improve understanding of the factors that influence disk dissipation and survival, our sample includes a wide range of complex and isolated star-forming regions. This comparison will differ from past studies of disk incidence in its greater sensitivity to faint objects, in its unbiased coverage of large cloud areas, and in its inclusion of isolated cores not in complexes.

3. Do "starless" isolated cores harbor faint protostars? Starless or "pre-protostellar" cores have no pointlike infrared emission, according to ground-based near-infrared observations and far-infrared observations by the *IRAS* and *ISO* satellites. These cores are prime targets for studies of the initial conditions of isolated star formation, and some such cores have associated internal motions suggestive of the early stages of star formation. *SIRTF*'s sensitivity will allow detection of extremely young protostars and proto–brown dwarfs missed by earlier observations. Identification of such objects would stimulate more detailed studies and so would advance our understanding of the earliest stage of star formation.

4. What are the statistical lifetimes of various stages? Our survey covers a large area and will catalog a large number of young and embedded systems. These data will allow the first unbiased statistical studies of the complete stellar content of five large clouds. In addition, systems that are statistically rare and systems in rapid phases of evolution will be present in the sample. We may, for example, find systems in the short-lived phase in which the first hydrostatic core forms, a crucial, but so far unobserved stage of star formation (Boss & Yorke 1995).

5. Do isolated cores with associated stars preferentially harbor single stars or small stellar groups? Observations by *IRAS* and *ISO* led to the idea of "one core, one star": an isolated core or globule tends to form a single star or an unresolved binary, as opposed to a small group of three to 10 members. In large molecular clouds, many isolated *IRAS* point sources are accompanied by groups of near-infrared sources that constitute the more evolved members of a small stellar group (e.g., Hodapp 1994). *SIRTF* will be much more sensitive to faint emission from nearby sources than were *IRAS* and *ISO*, allowing us to test whether truly isolated star formation occurs.

6. What is the density structure of individual cores? Some isolated starless cores have a density structure similar to that of a pressure-bounded isothermal sphere, according to observations of their submillimeter dust emission and of their near-infrared absorption of background starlight. These cores have a single local maximum of density and tend to make single stars. Line profiles toward these cores usually indicate low levels of turbulence. In contrast, cores in cluster-forming regions appear to have more complex density structure, and their spectral lines indicate more turbulent conditions. Deep IRAC imaging of such cores will reveal their detailed structure through mapping the extinction of background stars. This structure will be compared with that of isolated cores to improve understanding of the initial conditions for stellar groups.

2.2. Sample Selection

Our sample of the nearest star-forming molecular clouds covers a range of cloud "types" broad enough to encompass

[12] http://peggysue.as.utexas.edu/SIRTF.

all modes of star formation and sufficient in number to allow robust statistical conclusions. To ensure a wide variety of star-forming conditions, we target five large complexes known to be forming stars in isolation, in groups, and in clusters, and 156 small, isolated cores: 110 starless and 46 with associated *IRAS* sources.

The five large clouds selected for mapping, listed in Table 1, satisfy the following criteria: they contain a substantial mass of molecular gas, they are actively forming stars, they are within 350 pc, and they can be mapped in a reasonable amount of time. Table 1 gives for each target region the distance, the area to be mapped with IRAC, and the full time for IRAC and MIPS observations, including off-cloud comparison fields. Although the distance criterion excludes some important star-forming regions, such as the Orion clouds, it was imposed to ensure that our *SIRTF* observations would be sensitive to brown dwarfs. The Perseus cloud is the most distant cloud at 320 pc (de Zeeuw et al. 1999), although previous distance estimates range from 220 pc (Černis 1990) to 350 pc (Herbig & Jones 1983). The Taurus molecular cloud satisfies most criteria but is too large to be mapped within the time allocated.

The selected complexes span a wide range of conditions. The most quiescent and least opaque are Lupus and Chamaeleon II, whose young stars are isolated or in sparse groups, and whose gas has low extinction and narrow lines. The most turbulent complexes are Perseus, Ophiuchus, and Serpens, with more densely clustered stars. The guaranteed time observers (GTOs) will observe smaller regions in many of these clouds. Our goal is to provide complete and unbiased coverage down to a set A_V limit.

Selection of the compact molecular cores proceeded in three steps: selection of a large sample with inclusive criteria, classification into cores with and without known internal luminosity sources ("stars"), and reduction of the sample to eliminate objects being observed by GTOs and to fit within the allowed time. The latter requirement resulted in removing cores with less robust evidence for dense gas and dust. The initial criteria for selection of the isolated dense core sample were that the distance is less than 400 pc, that the size is not too large (typically less than 5′), and that the core has been mapped in a dense gas tracer, typically NH_3 (Jijina, Myers, & Adams 1999), CS (Lee, Myers, & Tafalla 2001), and/or N_2H^+ (Lee et al. 2001; Caselli et al. 2002). To supplement this list, we searched the ADS and astro-ph databases for other cores mapped in these tracers but not included in these catalogs, or mapped in other dense gas tracers, such as HCO^+, HCN, and H_2CO. We also added cores with dust continuum emission but without published maps in tracers of dense gas. Cores where more than one dense gas tracer had been detected, but no map exists, were added to include Bok globules, whose size can be estimated from their optical extinction.

To determine whether a core has an associated "star," meaning a central luminosity source at any evolutionary stage, we used the catalog of Lee & Myers (1999). For embedded sources (Class 0 and Class I), they searched the *IRAS* database and required the following to be true. The projected position of the *IRAS* source on the sky should fall within the contour of least extinction defining the optical extent of the core. The source should be detected in at least two wave bands. The detected flux densities (F) should be greater in the longer wavelength band. However, sources with $F_{100\,\mu m} < F_{60\,\mu m}$ or $F_{100\,\mu m} < F_{25\,\mu m}$ were included as long as $F_{60\,\mu m} > F_{25\,\mu m} > F_{12\,\mu m}$. To select pre–main-sequence stars from the *IRAS* catalog, the color-color criterion of Weintraub (1990) was used by Lee & Myers (1999), which requires $-2.00 < \log(\nu_{12}F_{12}/\nu_{25}F_{25})/\log(\nu_{12}/\nu_{25}) < 1.35$ and $-1.75 < \log(\nu_{25}F_{25}/\nu_{60}F_{60})/\log(\nu_{25}/\nu_{60}) < 2.20$. The Herbig & Bell (1988) catalog of pre–main-sequence stars was also searched. Other cores with stars were identified on a core-by-core basis from the literature; e.g., IRAM 04191+1522 was not detected by *IRAS* but was identified by its dust continuum emission (André, Motte, & Bacmann 1999) and found to have a central source.

TABLE 1
CLOUDS TO BE SURVEYED

Cloud	Distance (pc)	Area[a] (deg^2)	Time[b] (hr)
Perseus	320	3.8	52.7
Ophiuchus	125	8.0	78.1
Lupus	125	2.4	46.6
Serpens	310	0.8	12.9
Chamaeleon II	200	1.1	15.2

[a] Area mapped with IRAC; MIPS will cover a larger area.

[b] Time for full maps with IRAC and MIPS, including off-cloud comparison fields, using SPOT6.2.

This candidate target list was cross-checked against the GTO lists and the area to be mapped by us in the five large molecular clouds to remove overlap. In order to fit the time allocation, the list was further reduced by eliminating cores not detected at all in CS and N_2H^+, or detected, but not mapped, in a dense gas tracer and detected only weakly in millimeter or submillimeter continuum.

2.3. Planned Observations and Expected Results

The molecular cloud complexes and isolated cores will be observed with both IRAC and MIPS at all wavelengths from 3.6 to 160 μm, but we expect the 160 μm detector to be saturated toward these regions. Because most of the molecular clouds in our sample are at low ecliptic latitude ($-40° \le \beta \le 40°$), all observations will be made at two epochs separated by 3–6 hr in order to identify faint asteroids. One set of observations will be made in the high dynamic range mode of IRAC to minimize saturation on bright sources.

The boundaries for four of the five large cloud maps were defined using optical extinction maps from Cambrésy (1999) (see Figs. 1–4). A ^{13}CO map (Padoan et al. 1999; Fig. 5) was used to define the Perseus molecular cloud. The *SIRTF* map of Perseus will include nearly all of the area mapped in ^{13}CO; this region corresponds to $A_V \sim 2$, as inferred from maps of

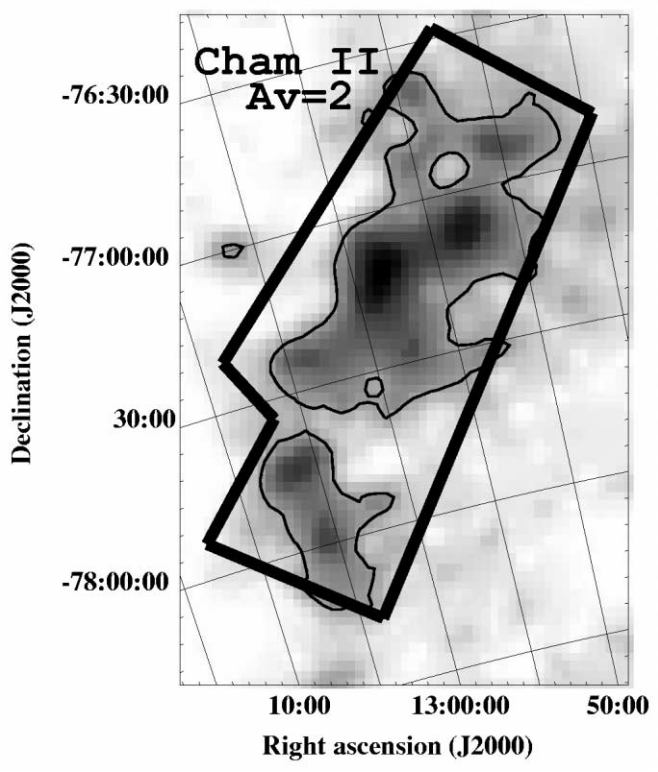

FIG. 1.—Observations for Chamaeleon II are outlined on this optical extinction map (Cambrésy 1999). The contour shows $A_V = 2$ and was used in planning.

near-infrared colors (J. M. Carpenter 2002, private communication) generated using the 2MASS Point Source Catalog (Cutri et al. 2001).[13] For the other clouds, an A_V level was chosen so that each map could cover a continuous area of high extinction within the allocated time. In most cases, $A_V = 2$ or 3 defined the cloud edge. However, the Serpens cloud boundary was limited to $A_V = 6$ because lower levels merge into unrelated extinction in the Galactic plane.

Several factors shaped the detailed observing strategy for the large clouds. In Ophiuchus and Perseus, some regions will saturate the MIPS 70 μm detector. Each saturated region was quarantined by limiting it to a single *SIRTF* astronomical observation request (AOR) so that the data in the surrounding regions would not be adversely affected. Point sources will also saturate; the afterimage may leave a trail in the direction of the MIPS scans. In order to obtain usable data in such regions, MIPS will scan in the opposite direction for the second-epoch observations. Additionally, many of our cloud maps overlap designated GTO regions. Therefore, unnecessary duplicate observations had to be avoided. Another factor considered in the observation planning was cloud orientation. The sky orientation of *SIRTF* maps for high ecliptic latitude targets, such as Chamaeleon II and Serpens, rotates rapidly. In order to eliminate the possibility of gaps in the maps due to this rotation, the overlap between adjacent AORs was increased, or the observations were constrained to specific position angles.

We also plan observations of off-cloud positions in order to sample properly the background source counts. In the selection of these off-positions, we implemented three criteria. First, in order to sample the stellar density gradient as a function of Galactic latitude, we chose off-cloud positions at different heights above the Galactic plane. Next, we required that $A_V < 0.5$ in the off-cloud regions, based on the optical extinction maps of Cambrésy (1999). Finally, the off-cloud regions were required to have little or no molecular emission (^{12}CO), based on the maps of Dame, Hartmann, & Thaddeus (2001). The off-cloud regions are mostly $15' \times 15'$. Using a Galactic model (Wainscoat et al. 1992), we have predicted the stellar background counts for each field (Table 2) and have chosen the size of the off-cloud region so that we will detect at least 100 background stellar sources at 3.6 μm. The counts in these off-cloud regions are often much greater than 100—e.g., at $b = 2°$ (for Serpens), we expect more than 10^5 background stellar counts in the $15' \times 15'$ region.

The cloud maps will be made using slightly overlapping IRAC frames and MIPS scan legs. The IRAC cloud maps will employ two dithers with an exposure time of 12 s in two epochs (24 s total). Since each cloud will be mapped twice, one map will be made in IRAC's high dynamic range (HDR) mode, which uses exposure times of 12 and 0.6 s, the shorter exposure time enabling photometry of bright point sources that might be saturated in the 12 s frames. Isolated clouds will be observed with the same parameters as large cloud complexes; expected sensitivities of the IRAC molecular cloud observations are given in Table 3.

The cloud area mapped with MIPS will be at least 20% larger than that mapped by IRAC because of the efficiency of MIPS scan mapping and the instrument-limited choice of scan lengths. Using the MIPS fast-scan mode, we will obtain 15 s exposures at each epoch and achieve the sensitivities given in Table 3. MIPS observations of isolated clouds will be made in large-source photometry mode. At 24 μm, an integration time of 3 s (for a total time, including two epochs, of 72 s) will be used. At 70 μm, isolated clouds that contain no *IRAS* sources, or *IRAS* sources fainter than 2 Jy at 60 μm, will be observed in the large-source, coarse-scale mode, with an integration time of 3 s (for a total time, including two epochs, of 36 s). Clouds that contain *IRAS* sources with 2 Jy $< S_\nu(60\ \mu\text{m}) < 10$ Jy will be observed at 70 μm in the large-source super-resolution mode (fine scale), with an integration time of 3 s (for a total time, including two epochs, of 48 s).

The 3 σ limits from Table 3 for the scan maps yield a limit on $L_{\rm bol}$ from 3.6 to 70 μm of about $10^{-3}\ L_\odot$ at 350 pc. Figure 6 shows (*clockwise from upper left*) the survey detection limits against typical spectral energy distributions for a heavily embedded protostar, a less embedded protostar with a disk, a brown dwarf with a disk of 4.5 $M_{\rm Jup}$, and an embedded brown dwarf. Our simulations indicate that disks as small as 1 $M_{\rm Earth}$

[13] http://www.ipac.caltech.edu/2mass.

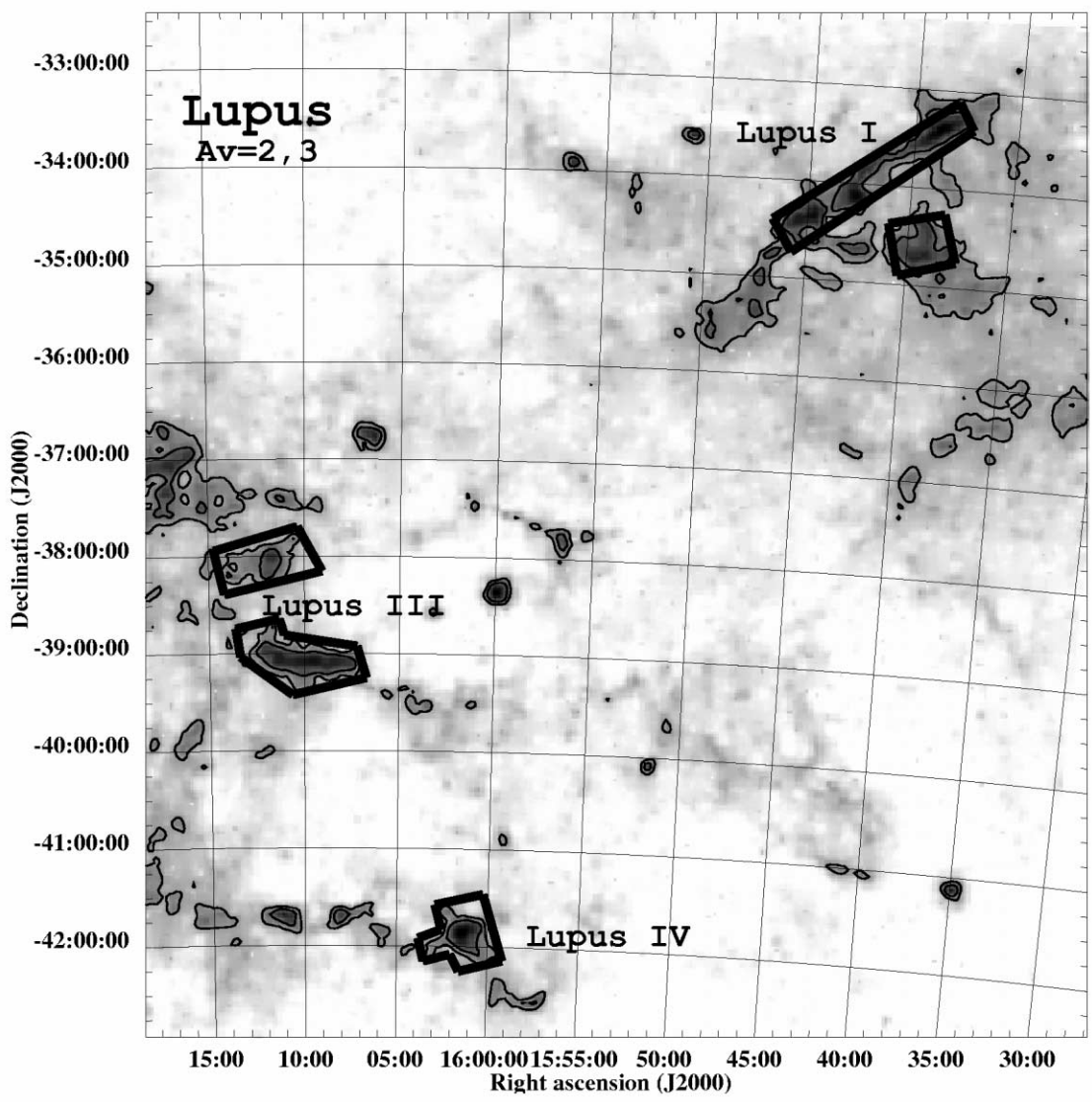

FIG. 2.—Planned observations of Lupus I, III, and IV based on the $A_V = 2$ contour (for III and IV) and the $A_V = 3$ contour (for Lupus I). The optical extinction map is from Cambrésy (1999).

could be detected, even when buried behind $A_V \approx 100$ mag of extinction. The IRAC bands would detect a 1 Myr old, 5 $M_{\rm Jup}$ brown dwarf at 350 pc, based on models by Burrows et al. (1997). The five large molecular complexes contain about 750 known stars and *IRAS* point sources. On the basis of recent estimates of the initial mass function in the field and in young clusters (Meyer et al. 2000; Luhman et al. 2000), we expect to identify several thousand new substellar objects. These must be distinguished from a large number of background stars (Table 2) and galaxies (e.g., Lagache, Dole, & Puget 2003) by color criteria (Fig. 6) and follow-up observations.

2.4. Ancillary and Complementary Data

To extend the data base to longer wavelengths, where the dust emission becomes optically thin and a good tracer of mass, we are obtaining ancillary data at millimeter wavelengths, using Bolocam for those clouds accessible from the Caltech Submillimeter Observatory (Perseus, Ophiuchus, and Serpens). In addition, we are obtaining complementary data for the southern clouds (Lupus and Chamaeleon) and isolated cores using the SEST Imaging Bolometer Array (SIMBA) on the Swedish-ESO Submillimeter Telescope (SEST). Further complementary data on the northern clouds in molecular lines and dust extinction and emission are being obtained by the COMPLETE[14] team, who also plan to make the data public.

Complementary data on the isolated cores are also being taken with the Submillimeter Common User Bolometric Array (SCUBA) on the James Clerk Maxwell Telescope (JCMT) and

[14] http://cfa-www.harvard.edu/agoodman/research8.html.

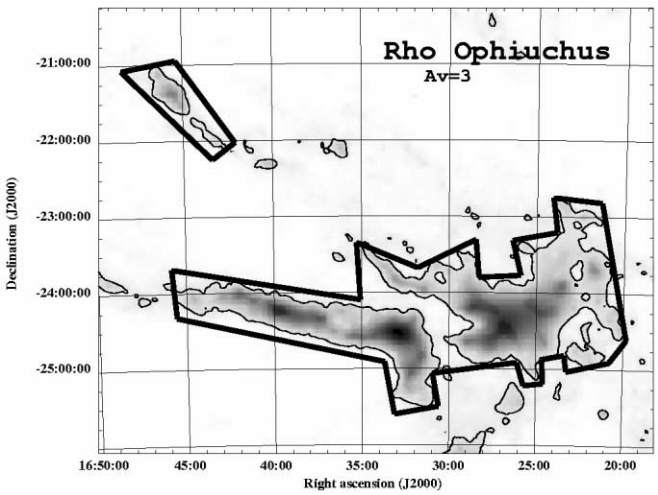

FIG. 3.—Planned observations for ρ Oph are outlined around the $A_V = 3$ contour (Cambrésy 1999).

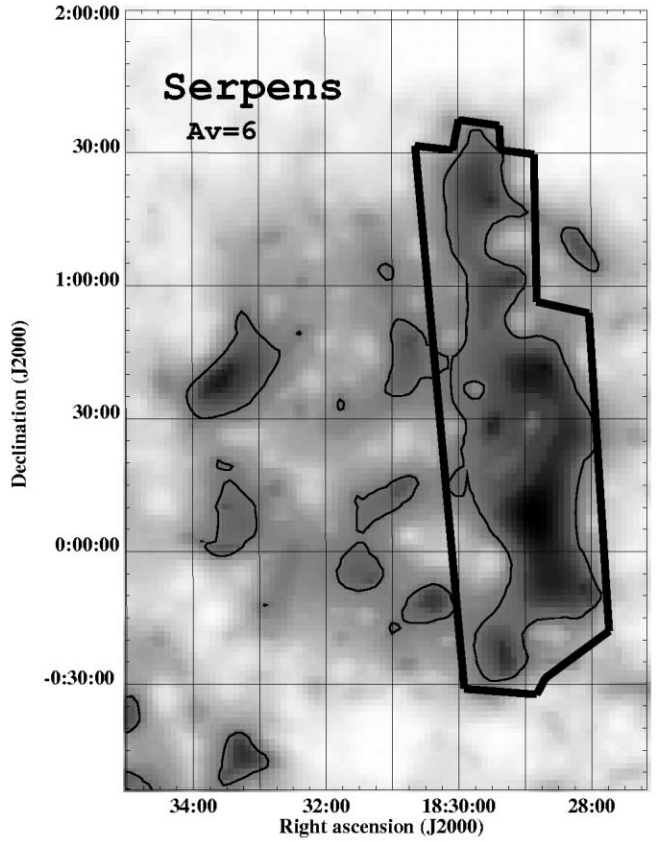

FIG. 4.—Planned observations for Serpens are outlined around the $A_V = 6$ contour (Cambrésy 1999).

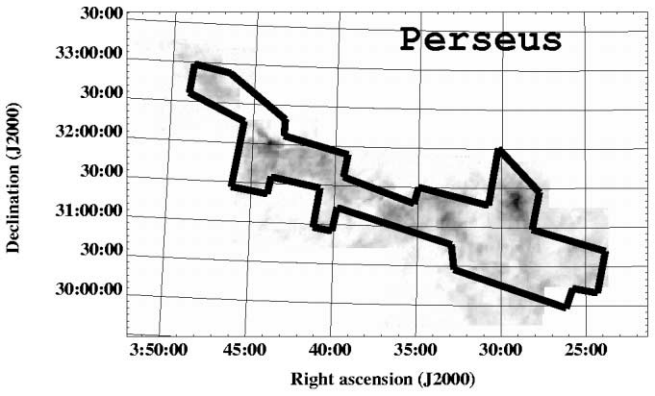

FIG. 5.—Observations of Perseus in ^{13}CO (*gray scale*) were primarily used in the *SIRTF* planning for this molecular cloud (Padoan et al. 1999). However, we also used maps of near-infrared colors from the 2MASS Point Source Catalog (Cutri et al. 2001) to provide constraints similar to those for the other clouds; the outlined region in this figure corresponds to $A_V \sim 2$.

MAMBO on the 30 m telescope of IRAM. Complementary spectral line data to extend the CS $J = 2 \rightarrow 1$ and N_2H^+ $J = 1 \rightarrow 0$ observations of Lee et al. (2001) and Caselli et al. (2002) are being obtained with the 32 element SEQUOIA focal-plane array on the Five College Radio Astronomy Observatory (FCRAO) 14 m telescope. These complementary data, which will be made available to the community through our c2d Web site, provide information on the existence and distribution of cloud material around objects detected at shorter wavelengths. Such information will be valuable for establishing the association of specific *SIRTF* sources with the cloud, for comparison of the material and stellar distributions, and for completing the overall picture of how star formation proceeds in clouds.

Complementary gas and dust observations on smaller scales are being acquired with the BIMA millimeter-wavelength array. A mapping survey of 21 embedded cores, mostly in the Perseus complex in the $\lambda = 2.7$ mm continuum and ^{13}CO and $C^{18}O$ $J = 1 \rightarrow 0$ lines, has been completed. The observed cores include well-known young embedded systems such as NGC 1333 IRAS 4, NGC 1333 IRAS 7, and B5 IRS 1, as well as ammonia cores without known embedded sources. The maps have a resolution of 2″ and a field of view of 100″. This combination of resolution and field of view will allow detailed comparisons of the gas, dust, and IRAC-derived stellar distributions. The

TABLE 2
EXPECTED STELLAR BACKGROUND COUNT

λ	Cha II	Lupus	Ophiuchus	Perseus	Serpens
L (3.6 μm)	400	7000	900	110	10^4
N (10.2 μm)	20	300	45	10	600
25 μm	1	8	1	1	15

NOTE.—Expected background counts are from the model of Wainscoat et al. 1992 and are for a 5′ × 5′ observing area. The wavelength bands do not exactly correspond to the *SIRTF* bands.

TABLE 3
SENSITIVITIES OF CLOUD SURVEY

λ (μm)	Sensitivity[a] (mJy)	Sensitivity[b] (mag)	Saturation (Jy)	Saturation (mag)
3.6	0.015	18.0	0.040	9.4
4.5	0.019	17.3	0.031	9.3
5.8	0.060	15.6	0.093	7.6
8.0	0.083	14.6	0.077	7.1
24	0.83	9.8	0.206	3.9
70	5.2	5.7	0.258	1.5

[a] Sensitivities are 3 σ for 24 s total time.
[b] Magnitudes based on power-law interpolation and extrapolation of zero-point fluxes from standard bands to the *SIRTF* wavelengths.

typical continuum sensitivity of 1 mJy beam^{-1} will permit detection of circumstellar disks down to a mass of 0.01 $M_{\odot}$. The molecular data will also provide velocity structure information, which can be used to look at the correlation between turbulent/systematic velocity fields and stellar binarity and the stellar spatial distribution.

In addition, as complementary data, the large clouds and many northern cores are being imaged at shorter (*R*, *i*, and *z*) wavelengths to limiting magnitudes of 24.5, 22, and 22, respectively. The photometry at these wavelengths will be very valuable for identifying young objects, discriminating against background and foreground stars, and extending the coverage of the spectral energy distribution. Extended objects will also be resolved, and young reflection nebulae and (contaminating) background galaxies will be identified. Data will be obtained primarily with the CFH12K and Megacam cameras at the Canada-France-Hawaii Telescope. Southern targets (such as Chamaeleon) will be imaged in similar bands with WFI at ESO, La Silla.

3. THE EVOLUTION OF DISKS UP TO 10 Myr

3.1. Scientific Questions

Disks around pre–main-sequence stars are the likely sites of planet formation. As such, they have been targets of extensive research over the past two decades. Surveys of continuum emission at infrared and millimeter wavelengths have established that 50% of all classical T Tauri stars (CTTSs; ages less than 3 Myr) have disks with typical masses of 10^{-3} to 10^{-1} $M_{\odot}$, sufficient to form a planetary system like our own (see Beckwith & Sargent 1996 and Beckwith 1999 for reviews). Disk sizes, as revealed by millimeter interferometry and *Hubble Space Telescope* (*HST*) images, range from 100 to 1000 AU in diameter. Much less is known about the occurrence and properties of disks in later stages of evolution. Evidence suggests that disk dispersal is marked by the termination of viscous accretion onto the star, dissipation of circumstellar gas, and the coagulation of grains into larger particles. During this process, disks are thought to evolve from an early opaque stage to one in which they are optically thin to both stellar radiation and their own thermal infrared emission. Examples of such "debris disks" are found in association with nearby stars at ages up to about 1 Gyr and contain relatively small amounts of dust (less than a few lunar masses). Analyses of timescales for grain dispersal have led to the conclusion that the dust is maintained by replenishment from asteroid collisions and cometary passages. The evolutionary transition between massive protoplanetary disks and tenuous debris disks appears to take place early in a star's life, perhaps within the first 10 Myr (Strom et al. 1989). However, the timescales and synchronization of dispersal processes are largely unknown.

Unprecedented sensitivity at critical wavelengths will enable *SIRTF* to address key questions in the early evolution of circumstellar disks. Weak-line T Tauri stars (WTTSs) represent a strategically important sample for this purpose. These young pre–main-sequence objects are characterized primarily by reduced signatures of protostellar accretion. In addition, they lack evidence for outflows and display diminished or absent near-infrared excess emission in contrast with their CTTS counterparts. *IRAS* and *ISO* detected far-infrared excesses in only a small fraction of WTTSs, but these early efforts lacked the sensitivity needed to detect the masses of material associated with nearby debris disks at the distances of the nearest star-forming clouds. Consequently, it remains unclear whether WTTSs are the evolutionary descendants of CTTSs or simply represent a population of stars *without* disks altogether. *SIRTF* studies of the WTTS population will bridge this gap in understanding and address the following key scientific questions:

1. What is the frequency of debris disks in the low-mass stellar population at ages of less than 5 Myr? Our program will establish the general presence or absence of disks in the WTTS sample together with the evolutionary implications of either possibility.

2. On what timescale does the metamorphosis from primordial to debris disk occur? By comparing CTTS and WTTS disk properties with those of the disks around young main-sequence stars in clusters, we can infer their evolutionary progress and synchronization. For example, grain-growth models predict a rapid transition from the opaque to translucent states, but the replenishment of small grains by planetesimal collisions may lead to a longer transition. The dispersion in disk properties within a coeval sample of stars will also provide a sensitive indicator of the diversity of evolutionary pathways for a forming planetary system.

3. Do most disks develop inner holes or gaps during the dissipation process? This aspect of disk structural evolution is observable through the signature of the spectral energy distribution, and our observations will indicate whether disk dissipation and planetesimal formation proceeds at an equal pace throughout the disk, or at an accelerated pace in the inner disk region.

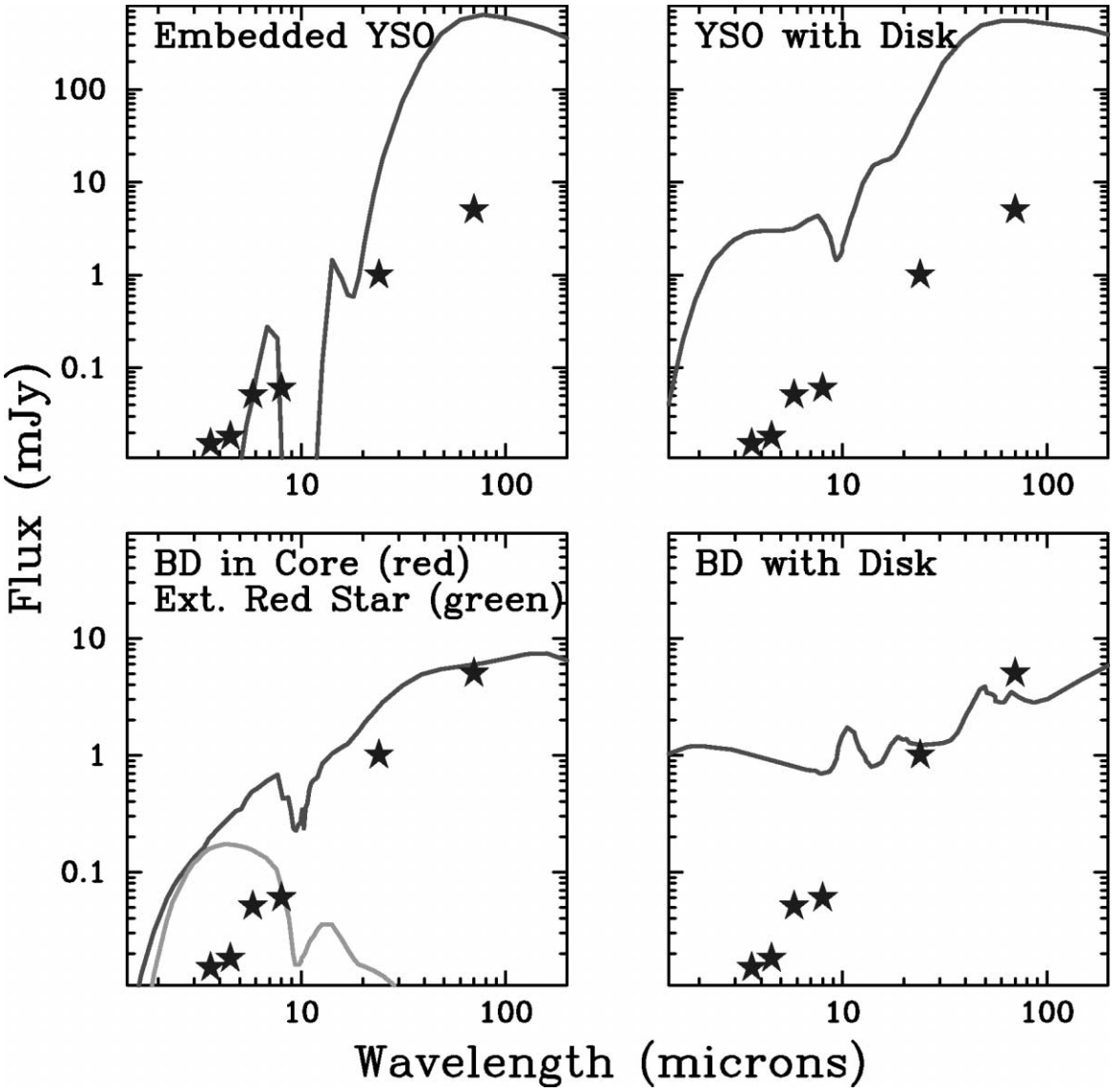

FIG. 6.—Flux density distributions for sources at 300 pc. Clockwise from upper left, a deeply embedded 0.1 $L_{\odot}$ protostar, a lightly embedded 0.1 $L_{\odot}$ star with a 30 AU circumstellar disk, a 10 Myr old 0.007 $L_{\odot}$ brown dwarf with a 4.5 $M_{\rm Jup}$ disk, and a young 0.003 $L_{\odot}$ brown dwarf with a 1 $M_{\rm Jup}$ envelope (E. Chiang et al. 2000, private communication). The lower curve in the lower left panel shows a background giant star with the same temperature, and with the same extinction, as the brown dwarf. The stars represent our 3 σ IRAC and MIPS sensitivity limits.

3.2. Sample Selection

The selection of WTTS targets was driven by three considerations. First, targets were sought that were associated with the large molecular clouds being mapped. The proper motion dispersion for WTTSs at 140 pc distance is sufficient for the stars to move several degrees away from their natal clouds on a timescale of 10 Myr (Hartmann et al. 1991), so targets were restricted to a zone within 5° from the cloud boundaries. Second, nearby WTTS targets were chosen because they allow the best sensitivity to dust excess. For this reason, only targets associated with clouds closer than 160 pc were considered. Third, we required that stars show evidence of young age: high levels of chromospheric activity as traced by X-ray emission detected by *ROSAT* and strong Li I 6707 Å absorption at levels exceeding those of Pleiades stars of the same spectral type.

On the basis of these criteria, we selected 190 targets associated with the Chamaeleon, Lupus, Ophiuchus, and Taurus clouds.[15] These are distributed as follows: 30 stars from Chamaeleon (Covino et al. 1997), 60 from Lupus (Wichmann et al. 1999), 40 from Ophiuchus (Martín et al. 1998), and 60 from

[15] Although the Taurus molecular cloud is not mapped by c2d, parts of the region are being mapped by *SIRTF* Guaranteed Time Observers and will be available for comparison.

Taurus (Wichmann et al. 2000). A few additional stars were selected from the catalog of Herbig & Bell (1988). Spectral types in the overall sample range from G5 to M5. Of the targets, 30 fall within the boundaries of the large cloud maps, leaving 160 to be measured separately. With the observing strategy outlined below, these 160 targets require 50 hr.

3.3. Planned Observations and Expected Results

We will search for excess infrared emission in our WTTS sample by means of photometric measurements at wavelengths[16] of 3.6, 4.5, 5.8, 8.0, 24, and 70 μm. At each target, single $5' \times 5'$ fields will be imaged with the IRAC and MIPS cameras. The IRAC observations consist of a single 0.6 s and two 12 s exposures. This sequence is designed to detect the stellar photospheres at signal-to-noise ratio (S/N) greater than 50 in all four IRAC bands. At 24 μm, the MIPS observation strategy will detect the stellar photosphere at an S/N level of 20. For the typical target, two photometry cycles with a 3 s exposure time are required to reach this sensitivity; actual exposure time will be tailored to the expected photospheric brightness of each star. At 70 μm, robust detection of a stellar photosphere would be prohibitively time consuming and probably impossible because of cirrus and extragalactic confusion. Consequently, we have aimed to achieve a more modest goal: S/N level greater than 5 for the detection of a β Pictoris–like debris disk characterized by a fractional luminosity of ~0.001 and 70 μm flux density 10 times the stellar photosphere. For the typical target, two photometry cycles with the 10 s exposure time are needed to achieve this. As at 24 μm, the planned exposure time is tailored to the brightness of the individual star.

The presence of infrared excess in an individual source can be readily determined by comparing its colors to those of *SIRTF* standard stars. To measure absolute levels of the excess, we will compare the observed flux densities to those of model photospheres appropriate to each object's spectral type, normalized to match available 2MASS photometry. Figure 7 shows how the survey sensitivity compares to the emission from various stars surrounded by a debris disk. The survey will readily detect disks similar to that around β Pic, even if they have evacuated inner holes with radii as large as 30 AU. Disks an order of magnitude more tenuous will still be detected if their inner edge is at a radius of 5 AU. Fitting of model spectral energy distributions to the *SIRTF* measurements will allow the disk optical depth, inner radius, and radial density/temperature profiles to be constrained.

3.4. Ancillary and Complementary Data

Two ground-based observing programs are being carried out in support of the c2d WTTS study. The first is ancillary echelle spectroscopy using the 4 m telescopes at the Kitt Peak National Observatory and the Cerro Tololo Inter-American Observatory. These spectra provide uniform measurements of spectral type, metallicity, lithium abundance, and chromospheric activity in the entire target sample, directly supporting the determinations of infrared excess and stellar age. The second is an adaptive optics (AO) search for source multiplicity using the ESO Adonis instrument (M. R. Hogerheijde et al. 2003, in preparation). The presence of companion stars has been shown to have a strong effect on the frequency of circumstellar disks (Jensen, Mathieu, & Fuller 1996); by understanding multiplicity in our sample, its effect on the disk properties can be isolated.

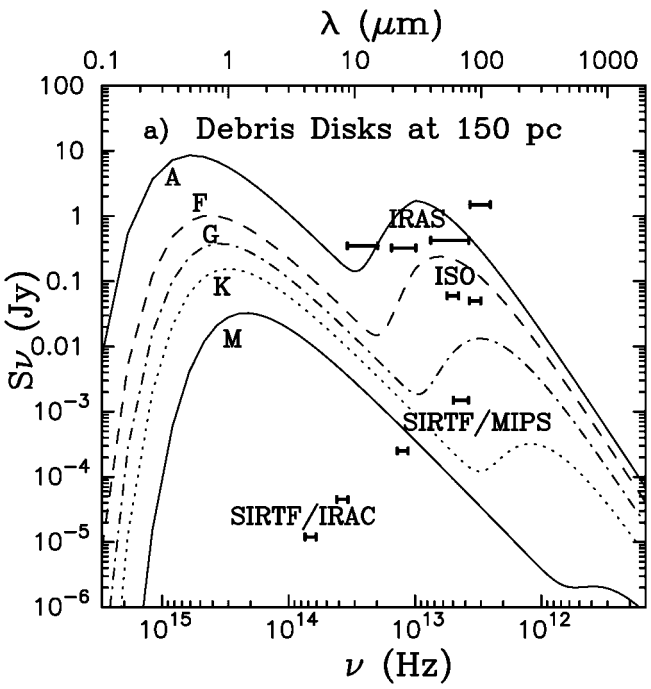

FIG. 7.—Flux density distributions for model debris disks around stars of various spectral types in nearby star-forming regions. Model properties are based on observations of debris disks around A stars, with 0.1 $M_{\rm Moon}$ of 30 μm sized dust grains in a zone extending from 30 to 60 AU radius. Horizontal bars mark 5 σ sensitivity levels for our survey and for *IRAS* and *ISO*.

4. THE EVOLUTION OF THE BUILDING BLOCKS OF PLANETS

4.1. Scientific Questions

Spectroscopy complements imaging and is essential for understanding the physical and chemical state and evolution of gas and dust surrounding young stellar objects. The mid-infrared wavelength range encompassed by *SIRTF* is particularly rich in diagnostic features, each of which probes different aspects of the star and planet formation process (see Table 4). Indeed, bands of solid-state material and the fundamental lines of the most abundant molecule, H_2, can be studied *only* in the

[16] While highly desirable, 160 μm photometry of our target sample is impractical because of the high sky backgrounds in the regions surrounding molecular clouds.

TABLE 4
SELECTED MID-INFRARED SPECTRAL FEATURES

λ (μm)	Species	Diagnostic
6.0	H_2O ice	Bulk of ice
6.2	PAH	UV radiation, carbonaceous material
6.8	Unidentified ice	Processed ices (UV/cosmic ray)
6.9	H_2 $S(5)$	Photon vs. shock heating
7.7	CH_4 ice	Building organics, solar system
7.7	PAH	UV radiation, carbonaceous material
8.0	H_2 $S(4)$	Photon vs. shock heating
8.6	PAH	UV radiation, carbonaceous material
9.7	Amorphous silicates	Bulk of dust
9.7	H_2 $S(3)$	Photon vs. shock heating
11.3	Mg_2SiO_4	Crystalline silicates, heating
11.3	PAH	UV radiation, carbonaceous material
12.2	H_2 $S(2)$	Temperature, ortho/para ratio
12.8	[Ne II]	Radiation field, shocks
15.2	CO_2 ice	Thermal history
15.6	[Ne III]	Radiation field
17.0	H_2 $S(1)$	Mass and temperature
18.5	(Mg, Fe)SiO_3	Crystalline pyroxenes
23.0	FeO	Oxides
25.2	[S I]	Shocks
27.5	Mg_2SiO_4	Crystalline silicates, heating
28.2	H_2 $S(0)$	Mass and temperature
33.5	Mg_2SiO_4	Crystalline silicates (enstatite)
35.8	Mg_2SiO_3	Crystalline pyroxenes
61	Crystalline H_2O	Crystalline ices, heating
70	Crystalline silicates	Crystalline silicates, heating

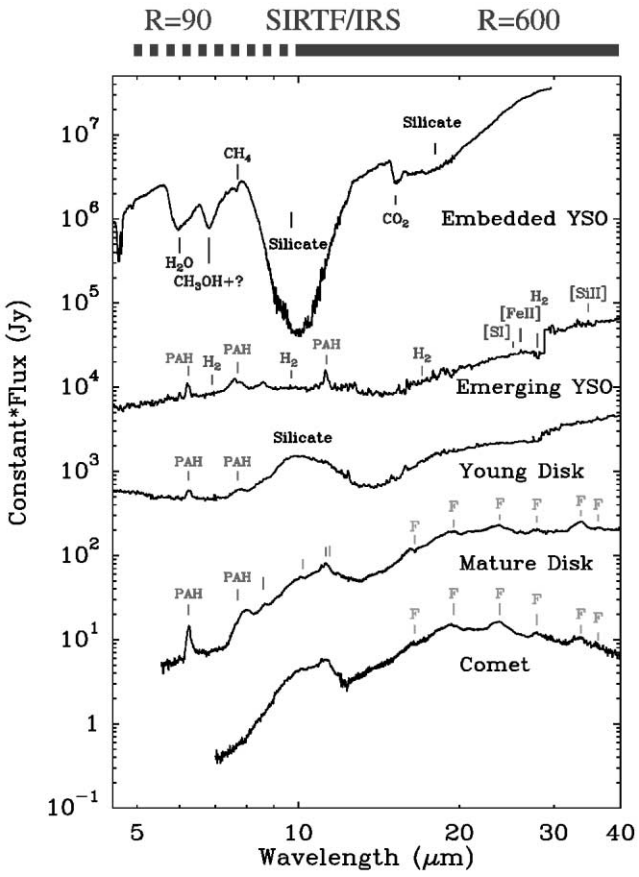

FIG. 8.—*ISO*-SWS mid-infrared spectra of newly formed stars in different stages of formation. From top to bottom (in a rough evolutionary sequence), the spectra change from dominated by solid-state absorption features (ices and amorphous silicates) to gas emission lines and PAH features to amorphous silicate emission and eventually crystalline silicate features (labeled "F"). Note the similarity of the spectra of mature disks with that of comet Hale-Bopp. *ISO* was able to obtain such spectra only for massive young stars; *SIRTF* has the capability to study these features for Sun-like objects. Based on van den Ancker et al. (2000a, 2000b), Gibb et al. (2000), Crovisier et al. (1997), and Malfait et al. (1998).

mid-infrared. In the 75 hr c2d IRS program, high-S/N spectra will be obtained over the full 5–40 μm range (high resolution [$R \approx 600$] over the 10–37 μm range) for all phases of star and planet formation up to ages of ~5 Myr for at least 170 sources. The MIPS-SED mode at 50–100 μm will also be used in the second year of the program to characterize the longer wavelength silicate and ice features of a disk subsample. Previous spectroscopic studies, e.g., with *ISO*, had the sensitivity to probe only high- or intermediate-mass young stellar objects. *SIRTF* will permit the first comprehensive mid-infrared spectroscopic survey of solar-type young stars.

The IRS spectra can be used to address the following questions:

1. What do spectroscopic diagnostics tell us about the different stages of early stellar evolution? As chronicled in Table 4 and Figure 8, there are many mid-infrared spectroscopic features that are potentially diagnostic for distinct physical and chemical states of young circumstellar environments. A classification based on these features would complement the current classification scheme (Lada & Wilking 1984) based on spectral energy distributions (SEDs). Prime diagnostics in the earliest embedded stages are the solid CO_2 bending mode at 15 μm, the [S I] 25 μm line and other atomic lines, the PAH features, and the H_2 lines. The shape of the 15 μm solid CO_2 band seen in absorption toward protostars is particularly sensitive to the thermal history of the envelope, and changes in its profile have allowed young high-mass protostars to be put in an evolutionary sequence (Gerakines et al. 1999). The [S I] 25 μm and H_2 lines probe the presence and properties of shocks, whereas the PAH features signal the importance of ultraviolet radiation. Together, they allow us to trace the relative importance of these two processes for clearing the envelope. A particularly exciting prospect is mid-infrared spectroscopy of disks as they are being unveiled.

In the later evolutionary stages, changes in silicate features become the main diagnostics. Indeed, one of the major results from the SWS instrument on *ISO* is that solid-state evolution of grain minerals occurs in disks around pre–main-sequence stars (Meeus et al. 2001). Some objects show only amorphous dust emission, whereas others have clear signatures of crystalline silicates and/or PAHs. These variations may be related

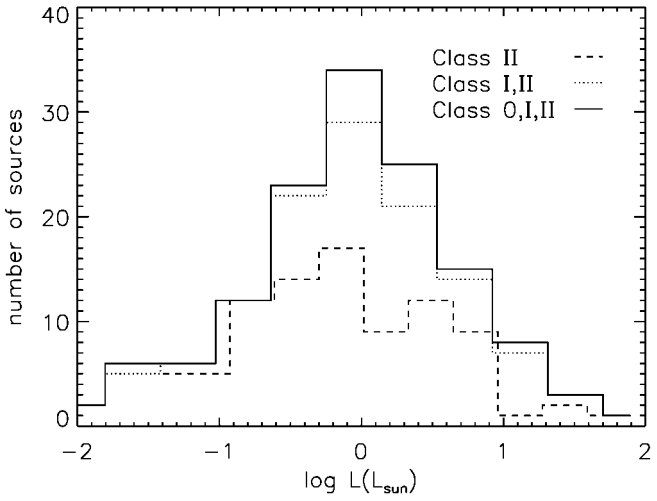

FIG. 9.—Distribution of luminosity over the sample for the first-look IRS observations. Stellar luminosities are calculated from fits to SEDs compiled from the literature (about 80% of sample is included in this plot).

to the processes of grain coagulation, settling, and destruction in the circumstellar disk, i.e., its evolution.

2. How does the chemical composition of dust and ices change from molecular clouds to planetary bodies? In the embedded phase, a reservoir of volatile and solid materials is delivered to the disk from the surrounding cloud core. The composition of the ices in the embedded phase can be probed by absorption spectroscopy, whereas that of the silicates in the pre–main-sequence phase requires emission studies. The low IRS resolving power below 10 μm does not allow detection of minor ice species, but the major ice components can be traced. Many ices may survive the accretion shock and will be incorporated into icy grain mantles in the outer reaches of planetary systems, perhaps to be delivered to inner planets intact. Indeed, remarkable similarities are found between the composition of interstellar ices and comets and between the crystalline silicates and PAHs seen in some disks and those in comet Hale-Bopp (Malfait et al. 1998). An inventory of the material present at each stage of low-mass envelope and disk evolution as a function of stellar luminosity, mass, and environment will be a major goal of the spectroscopy program. The resulting spectra will form a powerful database to compare with spectra of Kuiper belt objects, comets, and asteroids obtained in other *SIRTF* programs and to clarify the links between interstellar, circumstellar, and solar-system material.

3. How does the size distribution of dust grains evolve in circumstellar environments? Observational and theoretical evidence points to a great deal of activity in dust-grain evolution during the gas-rich disk phase, suggesting that grain growth to a kilometer-sized population of planetesimals may occur at this stage. The silicate emission widely observed from gas-rich disks arises from small ($\sim$0.5 μm) grains, while the underlying continuum stems from larger particles. Further, the overall excess shortward of 200 μm scales approximately as the ratio of the disk (dust) photosphere to the gas scale height (Chiang et al. 2001). The low-noise IRS spectra automatically cover the lowest pure rotational emission lines of H_2 at 28 and 17 μm, which may be detectable if the gas and dust temperatures are sufficiently different. Successful detection of these lines would permit an independent assessment of the dust coagulation and gas dissipation timescales, processes of great importance for planet formation.

It is important to note that the SEDs themselves do not give a unique answer to grain growth because of the degeneracy between disk mass and grain-size distribution in radiative transfer models, especially if the physical size of the disk is uncertain (Chiang et al. 2001). However, the combination of SEDs with complementary spatially resolved infrared and millimeter-wave images of disks does resolve the parameter correlation, making it possible to constrain the relative settling of the dust versus the gas in gas-rich disks and the earliest stages of planetesimal formation up to roughly millimeter sizes. Our c2d program will provide hundreds of objects for more detailed follow-up.

4. What is the spectral evolution of substellar objects? Do they form as stars do, or do they form as companions to stars? A clue that they form as stars do is the existence of a disk around many young substellar objects (Natta & Testi 2001; Apai et al. 2002; Liu, Najita, & Tokunaga 2003). Another important question is whether their atmospheres are dusty at later times. Atmospheric spectra are predicted to show significant changes with age and mass (e.g., Burrows et al. 1997). Apart from limited photometry, nearly nothing is known observationally about the mid-infrared spectra of brown dwarfs, young or old. The young brown dwarfs and super-Jupiters discovered in the IRAC and MIPS surveys ($\sim$ 100 expected) therefore form a critical second look population for study with the IRS.

4.2. Sample Selection

The IRS observations are divided into two sets with roughly equal time, the first being observations of known embedded and pre–main-sequence stars and the second consisting of follow-up spectroscopy of sources discovered in the IRAC and MIPS mapping surveys. The source list for the first-look program was restricted primarily to low-mass young stars, defined as having masses $M \lesssim 2\ M_{\odot}$ with ages younger than $\sim$5 Myr, for minimal overlap with existing infrared spectroscopy. Within these criteria, the selection contains a broad representative sample of young stars with ages down to 0.01 Myr and masses down to the hydrogen-burning limit or even less, if possible. Figure 9 shows the distribution of sources over luminosity, and Figure 10 shows the distribution over age.

The initial selection of sources to be observed with the IRS was constrained to the cloud regions scheduled to be mapped by IRAC. A large list of Class 0, I, and II sources was compiled, primarily from the existing near- and mid-infrared surveys of the mapped clouds (Persi et al. 2000; Bontemps et al. 2001).

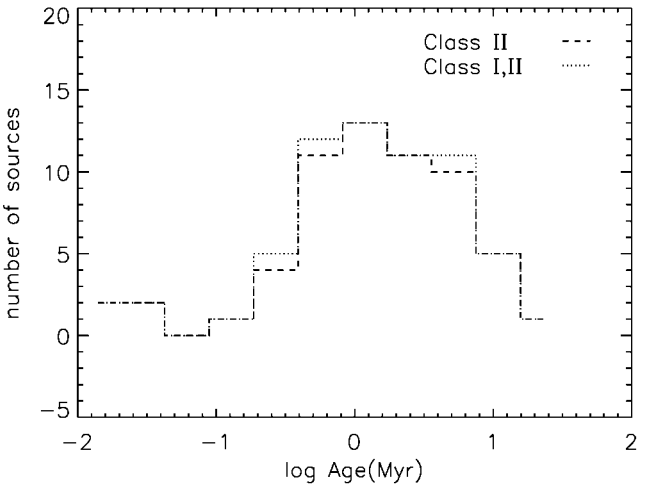

FIG. 10.—Distribution of ages over the sample for the first-look IRS observations. Note that age information is quite incomplete, and only $\frac{1}{4}$ of the sample is represented in this plot.

All overlaps with GTO high spectral resolution IRS targets were removed. The SIMBAD database was searched for additional observations and modeling of every source remaining in the list. All available photometric points were collected, and typical parameters such as bolometric luminosity, SED class, effective temperature, and optical extinction were entered into a concise database from which the final selection could be made. Stars with no measured mid-infrared fluxes were dropped first. The availability of sensitive ISOCAM surveys covering part of the mapped regions ensured that the fainter end of the luminosity function is well represented.

Most sources with 5–25 μm fluxes less than 200 mJy were also discarded in the first-look IRS sample because of time limitations; some fainter sources of special interest, such as a few stars known to have an edge-on disk, were retained. Stellar ages of the Class II sources were calculated by fitting the extinction-corrected temperature and bolometric luminosity from the database to the evolutionary tracks by Siess, Dufour, & Forestini (2000), assuming solar abundances. Stars with a calculated age of more than 5 Myr were subsequently discarded since systems of this age and older are covered in the FEPS Legacy spectrophotometry program, albeit largely at low spectral resolution. The flux limit to be achieved in the first-look survey corresponds to a typical source luminosity of 0.1 $L_{\odot}$ and mass of 0.1 $M_{\odot}$ in the Ophiuchus, Chamaeleon, Serpens, and Lupus clouds at an age of 1 Myr.

Care was taken at this point to verify that all stellar ages and masses within the limits of the full database were represented in the final sample. For completeness and comparison purposes, a few sources were added, such as background stars and certain Herbig Ae stars that were well characterized by the *ISO*-SWS. The final source list for the first-look survey consists of about 170 unique targets, of which about 10% belong to Class 0, 20% to Class I, and the rest to Class II. A roughly equal amount of time is reserved to the spectroscopic follow-up of interesting sources found in the imaging and photometry surveys, complementary MIPS-SED observations of selected first-look IRS sources, and spectral mapping of one cloud core.

4.3. Planned Observations and Expected Results

All first-look targets will be observed using the IRS staring mode in each of its four modules, except for those sources that are part of various GTO programs involving the low-resolution modules. For those stars, only the high-resolution 10–37 μm spectra will be acquired as part of the c2d IRS effort. Whenever possible, cluster observations will be used to reduce the slewing and peak-up overheads. Specifically, the moderate precision cluster mode will be used in conjunction with the blue filter on the peak-up array.

The integration times for the short-high and long-high modules were fixed such that theoretical S/Ns of at least 100 and 50 are obtained for sources brighter and fainter than 500 mJy, respectively. The spectra to be taken using the short-low modules always reach theoretical S/Ns of greater than 100. In contrast to the scheduled GTO observations of large numbers of young stars, typically with the low-resolution IRS modules, the c2d IRS program focuses on long integration times in the high-resolution modules, ensuring high dynamic range even on weak sources. Instrumental fringing may limit these S/Ns, so the c2d IRS team is leading the development of defringing tools for *SIRTF*, as described below. In order to evaluate the pointing performance of the spacecraft and assess the defringing software before beginning the full survey, the c2d IRS validation program will include cluster mode observations of stars with widely varying brightness.

While most of the objects will be observed in the IRS stare mode only, the northwestern Serpens molecular core will be imaged over more than 4 arcmin^2 to a 1 σ sensitivity of 2 mJy using the low-resolution IRS spectral mapping mode. This core contains several deeply embedded sources and possesses a complex physical structure with infall, outflow, and formation of the envelope and disk all occurring within 30″–60″ (~0.05–0.1 pc) of the central star. Because the continuum is weak off-source, emission lines can be detected even at $R = 60$–120, and every *SIRTF* pixel may have an interesting spectrum, ranging from those characterized by deep ice absorption bands toward the protostars themselves to silicate emission from nearby disk sources or strong ionized lines at the heads of shocks. At some positions, the "continuum" emission may even be entirely due to lines or PAHs, which could significantly affect the interpretation and classification of objects.

The targeted dynamic range of 50–100 on the continuum in the IRS stare observations is driven by the scientific questions outlined above, especially the desire to study the thermal history of the envelope through the 15 μm CO_2 bending-mode profiles and to search for gas-phase emission and absorption

TABLE 5
SUMMARY OF SAMPLES AND OBSERVATIONS

Item	Clouds	Cores	Disks	IRS Targets	Comments
Number	5	156	190	170+	First look[a]
Area (deg^2)	16	1	…	…	
IRAC	Map	Map	Photometry	…	3.6–8 μm
3.6 μm sensitivity	0.015	0.015	0.015	…	(mJy, 3 σ)
4.5 μm sensitivity	0.019	0.019	0.019	…	(mJy, 3 σ)
5.8 μm sensitivity	0.060	0.060	0.060	…	(mJy, 3 σ)
8.0 μm sensitivity	0.083	0.083	0.083	…	(mJy, 3 σ)
MIPS	Map	Map	Photometry	…	24, 70 μm
24 μm sensitivity	0.83	0.53	Varies[b]	…	(mJy, 3 σ)
70 μm sensitivity	5.2	4.7	Varies[b]	…	(mJy, 3 σ)
IRS	Select[c]	Select[c]	…	Low, high[d]	
S/N	50–100	50–100	…	50–100	On continuum
Complementary	Yes	Yes	Yes	Yes	Ancillary as noted
Visible images	Map	Select[c]	…	…	*R*, *i*, *z* images
Visible spectra	…	…	190	…	Ancillary
NIR AO	…	…	Select[c]	…	Adaptive optics
MIR spectra	Select[c]	Select[c]	…	Select[c]	
Millimeter/submillimeter[e]	Map	Map	…	Select[c]	Continuum maps
Millimeter interferometry[f]	Select[c]	…	…	Select[c]	Continuum maps
Millimeter spectra	Map	Map	…	Select[c]	Spectral maps

[a] A roughly similar number of spectral sources will be observed in second-look mode, based on the results of the continuum surveys.

[b] Adjusted to achieve a certain S/N depending on the star.

[c] Selected objects or regions within this sample will be observed in the indicated mode; the coverage is not complete. For example, 129 of the IRS targets are toward the large clouds.

[d] Spectra will be taken with both low resolving power ($R \approx 60$–120) and high resolving power ($R \approx 600$) modules.

[e] Large-scale maps made with bolometer arrays (Bolocam, SIMBA, SCUBA, MAMBO). Maps of three clouds (Perseus, Ophiuchus, and Serpens) are ancillary data.

[f] Small-scale maps of selected regions made with interferometers (BIMA, OVRO).

features in all phases of star formation. Even at $R = 600$, however, minor grain mantle components will be difficult to detect, and little or no kinematic information will be gleaned from the gas-phase lines. In addition, no information will be available on features shortward of 5 μm.

4.4. Complementary Data

As a complementary ground-based program, we have therefore initiated flux-limited surveys in the atmospheric *L*-band and *M*-band windows using the VLT-ISAAC and Keck NIRSPEC (McLean et al. 1998) instruments in order to examine the fundamental stretching vibrations of the H_2O and CO molecules, respectively. The excellent sensitivity of these spectrometers has enabled the first high spectral resolution ($R =$ 10,000–25,000) CO observations of low-mass protostars, revealing both gaseous and solid CO (Pontoppidan et al. 2003). Embedded sources in Taurus and Ophiuchus show a blend of gas-phase CO absorption and emission profiles that are related to the simultaneous infall and outflow velocity fields in protostars (see Pontoppidan et al. 2002). Studies of edge-on disk sources have been particularly revealing of the solid-state components and velocity fields in accretion disk surface layers and midplane (Boogert, Hogerheijde, & Blake 2002a; Thi et al. 2002). In older Class II disk systems, particularly Herbig Ae stars, emission from CO and atomic hydrogen lines is observed and likely arises from the inner disk in or near the dust sublimation radius (see also Dullemond, Dominik, & Natta 2001; Brittain & Rettig 2002).

A subset of IRS targets with known infrared ice absorption features is being characterized, using the CSO and OVRO facilities. Observations of $C^{18}O$ and HCO^+ lines as well as millimeter continuum emission are used to derive the distribution and physical conditions (temperature, density, and column density) of material along the line of sight. This information is crucial in locating the ices and understanding ice evolution indicators (ice column, absorption-band profile), as well as in properly interpreting the spectral energy distribution (Boogert et al. 2002b).

4.5. Analysis Tools

The c2d-IRS team will enhance the IRS pipeline data delivered by the SSC in several ways. The most important improvement will be in the defringing of the IRS spectra, because laboratory experiments indeed show the presence of fringes. Special software derived from the *ISO*-SWS experience is being written for defringing both one-dimensional and two-dimen-

TABLE 6
ANTICIPATED DATA PRODUCTS AND DELIVERY DATES

Date	Product	If Observed By[a]
$L + 9$	Sampler: validation observations, all modes	$L + 6$
	Ancillary NOAO optical spectroscopy of WTTSs	...
	Catalog of IRAC/MIPS results for WTTSs	$L + 6$
$L + 15$	Initial band-merged, cross-identified catalog for WTTSs	$L + 12$
	Initial band-merged, cross-identified catalog for cores	$L + 12$
	ECDs for cores, cloud areas	$L + 12$
	Spectra, cataloged features, first-look targets	$L + 12$
$L + 21$	Final band-merged, cross-identified catalog for WTTSs	$L + 15$
	Final band-merged, cross-identified catalog for cores	$L + 15$
	Mosaics for cores	$L + 15$
	Mosaic for Cha II	$L + 15$
	Defringed spectra, cataloged features, first look	$L + 15$
$L + 27$	Mosaics for clouds	$L + 9$[b]
	Final band-merged, cross-identified catalog for clouds	$L + 9$[a]
	Ancillary submillimeter cloud maps	$L + 9$[b]
	Catalog of small extended sources	$L + 9$[b]
	Catalog of transient sources	$L + 9$[b]
	Defringed spectra, cataloged features, second look	$L + 24$
$L + 31$	Mosaics for any delayed clouds	$L + 12$[b]
	Updated catalogs for any delayed clouds	$L + 12$[b]
	Defringed spectra, cataloged features, second look	$L + 28$
	Complementary data, where possible	...

NOTE.—The products and delivery dates are based on assuming that the spacecraft and all instruments function normally and that the data pipeline runs smoothly. If any of those assumptions are wrong, products may be delayed or even eliminated. The dates are all given in months after launch (L).

[a] Products will be available on sources observed by this date.

[b] All large clouds except Cha II have "cutouts," areas observed by GTOs; these areas will not be available to us until 12 months after they are observed. Delivery of our final cloud images and catalogs depends on the observation date of these cutouts.

sional spectra (Lahuis & Boogert 2003). The in-flight fringe characteristics (complexity and amplitude) are presently unknown, however, which is one of the reasons why two independent defringing approaches, each with its own merits, are being exploited. The first uses a robust method of iteratively fitting sine functions; the second algorithm minimizes fringe residuals by correcting the flat field to best match the data. In parallel, a "complete" fringe model is being developed, applying basic optical theory and incorporating the geometry and optical properties of the IRS detectors. The routines are written in IDL, and the resulting modules are compatible with the SMART package, developed by the IRS instrument team for their data reduction and management.[17] The one-dimensional prelaunch modules have been delivered to the SSC for use by the community. Other improvements to the pipeline data will come from monitoring of the data quality and calibration over time.

5. DATA PRODUCTS

The source samples and observations are summarized in Table 5. The data products (summarized in Table 6) include the following categories of observations and analyses: *SIRTF* mapping observations together with an associated source catalog and ancillary mapping of the same regions at millimeter wavelengths, *SIRTF* photometry and NOAO optical spectroscopy of associated WTTSs, and IRS spectroscopy of a sample of objects at all stages of early evolution. These data can be used by the community to address far more than just the principal science areas listed above. We describe the particulars of these products below in hopes that other researchers will easily recognize their utility across a broader range of scientific studies. *SIRTF* and ancillary products will be made available to the *SIRTF* Science Center for community access through the Infrared Sky Archive (IRSA). Because the complementary data are being obtained by many researchers operating under many different guidelines about archiving, the availability of those data will be handled on a case-by-case basis. We hope to make most of the complementary data accessible eventually, through either IRSA or our Web sites.

5.1. Clouds and Cores

We will examine and, where necessary, enhance the basic calibrated data (BCD) delivered by the pipeline at the *SIRTF* Science Center. We will provide to IRSA the enhanced calibrated data (ECD) for all the fields incorporated in our IRAC

[17] See http://www.astro.cornell.edu/SIRTF.

and MIPS imaging studies of nearby star-forming regions. In addition, we will provide mosaicked maps of the clouds and cores; these products are referred to in Table 6 as mosaics. A band-merged catalog of sources contained within these images will also be compiled and provided to IRSA. The catalog will include cross-identifications with known pre–main-sequence objects, foreground stars, and transient sources (for example, asteroids in the field of view). This resource should allow the community easy access to *SIRTF* photometry of any individual objects that fall within our field of view, as well as the capability to carry out statistical studies of color- or magnitude-selected samples with the help of the IRSA search engine. As noted in Table 6, all of our large clouds except Cha II include "cutouts," regions observed by GTOs. Because data on these regions will not be available to us until 12 months after they are observed, delivery of full mosaics and catalogs for those clouds will depend on the observation date of those cutouts.

5.2. Data Products for Weak-Line T Tauri Stars

IRAC and MIPS images of WTTSs will be processed in the same manner as the images of isolated cloud cores and extended molecular clouds and the results provided to IRSA. The c2d team will also deliver the following: (1) ECD consisting of images in six *SIRTF* bands; (2) a catalog of the sample that includes cross-identifications with observations in the literature and spectral energy distributions including both *SIRTF* and published measurements; (3) new high-resolution optical spectra for the sample, together with derivative properties, such as equivalent widths of lithium and Hα, and with radial velocities and identification of any double-lined spectroscopic binaries; and (4) a list of positions and fluxes for serendipitous sources. Archival researchers will be able to access *SIRTF* photometry, band-merged with other relevant photometric measurements for any individual source of interest, or to view selected properties of the entire sample with the help of IRSA.

5.3. IRS Data Products

The data products will consist of best-effort reduced and defringed spectra, together with an identification of the spectral features where possible. Results from our complementary VLT, Keck, and CSO/SEST programs will be made available through publications in refereed journals. The reduced spectra will appear on the c2d Web site at the time of the final data delivery from our program.

The most important improvement the c2d-IRS team will make to the IRS pipeline data is defringing of the spectra. Special software has been written for this purpose (§ 4.4). The one-dimensional prelaunch modules have been delivered to the SSC for use by the community. Other improvements to the pipeline data will come from monitoring of the data quality and calibration over time.

5.4. Modeling Tools

Simple modeling tools that fit the photometric data of individual sources with emission from protostellar cores and circumstellar disks will be available to help identify the nature of cataloged sources.[18] Simple analysis programs for modeling SEDs from disks are being developed for our team based on the formalism by Dullemond et al. (2001) and will be made available through the c2d Web site.

6. SUMMARY

The c2d program will provide a legacy for future research on star and planet formation. By selecting samples with attention to coverage of the relevant parameters, we hope to provide a database for unbiased statistical studies of the formation of stars and substellar objects. Ancillary and complementary data from other wavelength regimes will complete the picture. Analysis and modeling tools will assist researchers in getting the most out of the database. The source lists may be found on the c2d Web page, noted in the introduction, by following the link to "source list." Table 5 summarizes the samples (columns) and observations (rows) to be collected, and Table 6 lists the data products and anticipated delivery dates. Of course, source lists, observations, data products, and delivery dates may be modified if in-flight performance differs from what was predicted.

We anticipate extensive follow-up studies of these samples with *SIRTF* itself and with future missions such as *SIM*, *Herschel*, *SOFIA*, *JWST*, and *TPF/Darwin*, as well as with ground-based instruments such as SMA, CARMA, and ALMA.

This research has made use of NASA's Astrophysics Data System, the SIMBAD database, operated at CDS, Strasbourg, France, and the NASA/IPAC Infrared Science Archive, which is operated by the Jet Propulsion Laboratory, California Institute of Technology, under contract with the National Aeronautics and Space Administration. We thank L. Cambrésy and P. Padoan for supplying electronic versions of data. Support for this work, part of the *Space Infrared Telescope Facility* (*SIRTF*) Legacy Science Program, was provided by NASA through an award issued by the Jet Propulsion Laboratory, California Institute of Technology, under NASA contract 1407. The Leiden *SIRTF* legacy team is supported by a Spinoza grant from the Netherlands Foundation for Scientific Research (NWO) and by a grant from the Netherlands Research School for Astronomy (NOVA). C. W. L. is partially supported by grant R01-2000-000-00025-0 from the Basic Research Program of the Korea Science and Engineering Foundation.

[18] http://wits.ipac.caltech.edu.

REFERENCES

André, P., Motte, F., & Bacmann, A. 1999, ApJ, 513, L57
Apai, D., Pascucci, I., Henning, T., Sterzik, M. F., Klein, R., Semenov, D., Günther, E., & Stecklum, B. 2002, ApJ, 573, L115
Beckwith, S. V. W. 1999, in NATO ASI Ser. C, 540, The Origin of Stars and Planetary Systems, ed. C. J. Lada & N. D. Kylafis (Boston: Kluwer), 579
Beckwith, S. V. W., & Sargent, A. I. 1996, Nature, 383, 139
Bontemps, S., et al. 2001, A&A, 372, 173
Boogert, A. C. A., Hogerheijde, M. R., & Blake, G. A. 2002a, ApJ, 568, 761
Boogert, A. C. A., Hogerheijde, M. R., Ceccarelli, C., Tielens, A. G. G. M., van Dishoeck, E. F., Blake, G. A., Latter, W. B., & Motte, F. 2002b, ApJ, 570, 708
Boss, A. P., & Yorke, H. 1995, ApJ, 439, L55
Brittain, S. D., & Rettig, T. 2002, Nature, 418, 57
Burrows, A., et al. 1997, ApJ, 491, 856
Cambrésy, L. 1999, A&A, 345, 965
Caselli, P., Benson, P. J., Myers, P. C., & Tafalla, M. 2002, ApJ, 572, 238
Černis, K. 1990, Ap&SS, 166, 315
Chiang, E. I., Joung, M. K., Creech-Eakman, M. J., Qi, C., Kessler, J. E., Blake, G. A., & van Dishoeck, E. F. 2001, ApJ, 547, 1077
Covino, E., Alcala, J. M., Allain, S., Bouvier, J., Terranegra, L., & Krautter, J. 1997, A&A, 328, 187
Crovisier, J., Leech, K., Bockelee-Morvan, D., Brooke, T. Y., Hanner, M. S., Altieri, B., Keller, H. U., & Lellouch, E. 1997, Science, 275, 1904
Cutri, R. M., et al. 2001, Explanatory Supplement to the 2MASS Second Incremental Data Release (Pasadena: Caltech)
Dame, T. M., Hartmann, D., & Thaddeus, P. 2001, ApJ, 547, 792
de Zeeuw, P. T., Hoogerwerf, R., de Bruijne, J. H. J., Brown, A. G. A., & Blaauw, A. 1999, AJ, 117, 354
Dullemond, C. P., Dominik, C., & Natta, A. 2001, ApJ, 560, 957
Engelbracht, C. W., Young, E. T., Rieke, G. H., Rivlis, G., Beeman, J. W., & Haller, E. E. 2000, Exp. Astron., 10, 403
Fazio, G. G., et al. 1998, Proc. SPIE, 3354, 1024
Gallagher, D. B., Irace, W. R., & Werner, M. W. 2003, Proc. SPIE, 4850, 17
Gerakines, P. A., et al. 1999, ApJ, 522, 357
Gibb, E., et al. 2000, ApJ, 536, 347
Hartmann, L., Stauffer, J. R., Kenyon, S. J., & Jones, B. F. 1991, AJ, 101, 1050
Herbig, G. H., & Bell, K. R. 1988, Lick Obs. Bull. 1111
Herbig, G. H., & Jones, B. F. 1983, AJ, 88, 1040
Hodapp, K. 1994, ApJS, 94, 615
Houck, J., van Cleve, J., Brandl, B., Charmandaris, V., Devost, D., & Uchida, K. 2000, in 2nd *ISO* Workshop on Analytical Spectroscopy: *ISO* beyond the Peaks, ed. A. Salama, M. F. Kessler, K. Leech, & B. Schulz (ESA-SP 456; Paris: ESA), 357
Jensen, E. L., Mathieu, R. D., & Fuller, G. A. 1996, ApJ, 458, 312
Jijina, J., Myers, P. C., & Adams, F. C. 1999, ApJS, 125, 161
Lada, C. J., & Wilking, B. A. 1984, ApJ, 287, 610
Lagache, G., Dole, H., & Puget, J.-L. 2003, MNRAS, 338, 555
Lahuis, F., & Boogert, A. C. A. 2003, in Proc. Waterloo Conf., Chemistry as a Diagnostic of Star Formation, ed. M. Fich et al. (Ottawa: NRC Press), in press
Lee, C. W., & Myers, P. C. 1999, ApJS, 123, 233
Lee, C. W., Myers, P. C., & Tafalla, M. 2001, ApJS, 136, 703
Liu, M. C., Najita, J., & Tokunaga, A. T. 2003, ApJ, 585, 372
Luhman, K. L., Rieke, G. H., Young, E. T., Cotera, A. S., Chen, H., Rieke, M. J., Schneider, G., & Thompson, R. I. 2000, ApJ, 540, 1016
Malfait, K., Waelkens, C., Waters, L. B. F. M., Vandenbussche, B., Huygen, E., & de Graauw, M. S. 1998, A&A, 332, L25
Martín, E., Montmerle, T., Gregorio-Hetem, J., & Casanova, S. 1998, MNRAS, 300, 733
McLean, I. S., et al. 1998, Proc. SPIE, 3354, 566
Meeus, G., Waters, L. B. F. M., Bouwman, J., van den Ancker, M. E., Waelkens, C., & Malfait, K. 2001, A&A, 365, 476
Meyer, M. R., Adams, F. C., Hillenbrand, L. A., Carpenter, J. M., & Larson, R. B. 2000, in Protostars and Planets IV, ed. V. Mannings, A. P. Boss, & S. S. Russell (Tucson: Univ. Arizona Press), 121
Natta, A., & Testi, L. 2001, A&A, 376, L22
Padoan, P., Bally, J., Billawala, Y., Juvela, M., & Nordlund, Å. 1999, ApJ, 525, 318
Persi, P., et al. 2000, A&A, 357, 219
Pontoppidan, K. M., Schöier, F. L., van Dishoeck, E. F., & Dartois, E. 2002, A&A, 393, 585
Pontoppidan, K. M., et al. 2003, A&A, submitted
Siess, L., Dufour, E., & Forestini, M. 2000, A&A, 358, 593
Strom, K. M., Strom, S. E., Edwards, S., Cabrit, S., & Skrutskie, M. F. 1989, AJ, 97, 1451
Thi, W. F., Pontoppidan, K. M., van Dishoeck, E. F., Dartois, E., & d'Hendecourt, L. 2002, A&A, 394, L27
van den Ancker, M. E., Bouwman, J., Wesselius, P. R., Waters, L. B. F. M., Dougherty, S. M., & van Dishoeck, E. F. 2000a, A&A, 357, 325
van den Ancker, M. E., Wesselius, P. R., & Tielens, A. G. G. M. 2000b, A&A, 355, 194
Wainscoat, R. J., Cohen, M., Volk, K., Walker, H. J., & Schwartz, D. E. 1992, ApJS, 83, 111
Weintraub, D. A. 1990, ApJS, 74, 575
Wichmann, R., Covino, E., Alcala, J. M., Krautter, J., Allain, S., & Hauschildt, P. H. 1999, MNRAS, 307, 909
Wichmann, R., et al. 2000, A&A, 359, 181